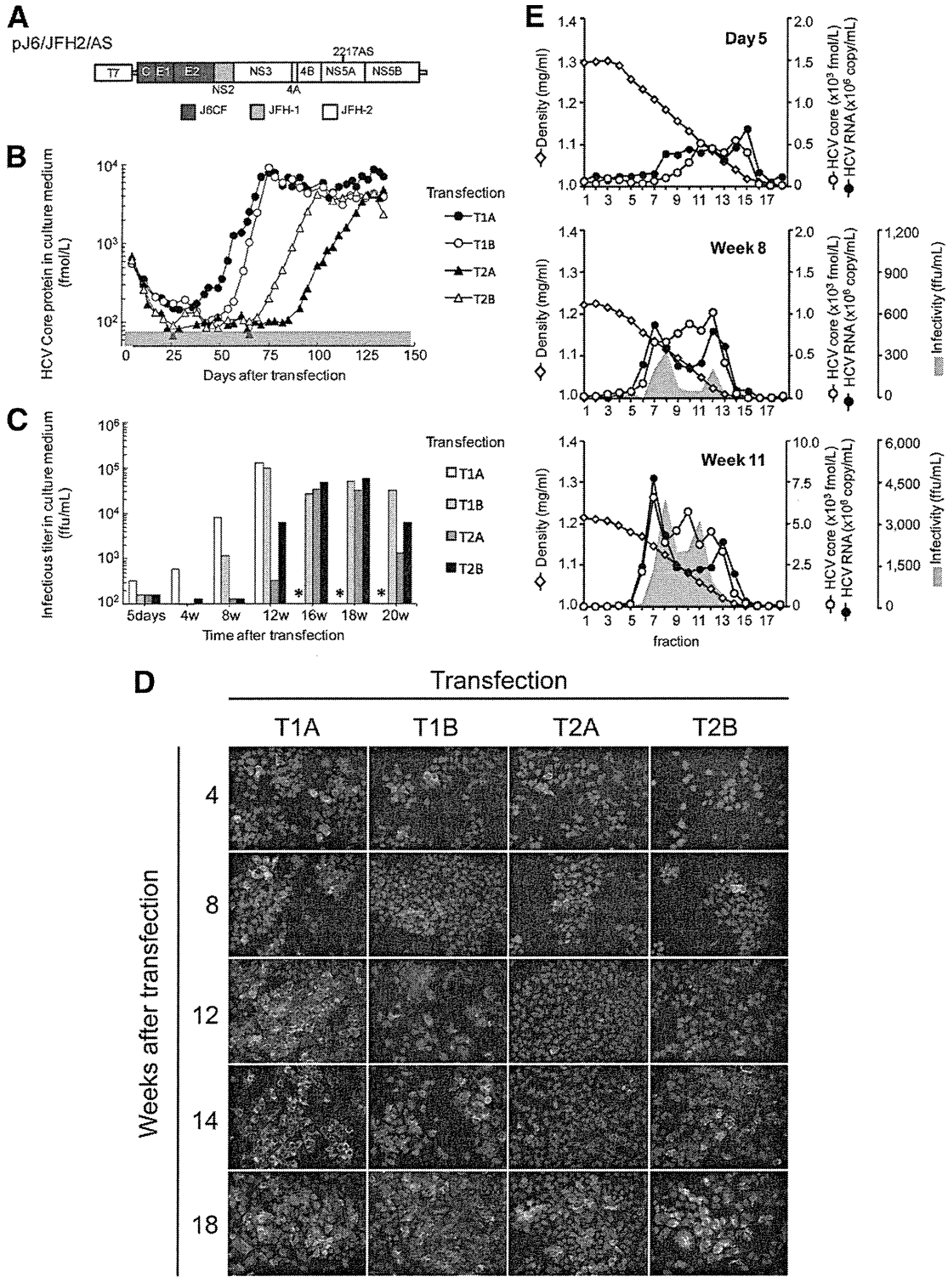

FIG 6 J6/JFH2 chimeric full-length HCV replication. (A) Organization of full-length chimeric JFH-2 construct, pJ6/JFH2/AS. A T7 RNA promoter is located upstream of the 5′ end of the HCV cDNA construct. The 5′ UTR and NS2 region are derived from the JFH-1 strain. Regions of the core protein to E2/p7 are derived from the J6CF strain. The 2217AS adaptive mutation is introduced. (B) Huh-7.5.1 cells were transfected with the transcribed RNA from pJ6/JFH2/AS. Two independently transfected cell lines (transfections 1 and 2 [T1 and T2, respectively]) were divided into two passages, resulting in four independently passaged transfected cell lines (T1A, T1B, T2A, and T2B). At each time point, culture medium was harvested and analyzed for the presence of HCV core protein by Lumipulse Ortho HCV Ag (Ortho-Clinical Diagnostics). The gray area indicates values that are below the detection limit. (C) Infectious titers in the culture supernatant of the passaged transfected cells (T1A, T1B, T2A, and T2B) were determined by focus formation assay. After 16 weeks, the culture media from T1A

TABLE 4 Specific infectivity of culture medium after transfection of J6/JFH2/AS RNA

Cell culture medium (no. of days posttransfection)	Infectivity (FFU/ml)	HCV core protein (fmol/liter)	HCV RNA (no. of copies/ml)	Specific infectivity	
				Infectivity/HCV core protein	Infectivity/HCV RNA (10^4)
T1A (5)	3.20E+1	3.57E+2	2.63E+6	0.09	0.12
T1B (5)	1.60E+1	3.07E+2	2.35E+6	0.05	0.07
T2A (5)	1.60E+1	3.13E+2	2.99E+6	0.05	0.05
T2B (5)	1.60E+1	2.63E+2	3.42E+6	0.06	0.05
T1A (82)	1.28E+4	5.47E+3	2.63E+7	2.34	4.87
T1B (82)	9.83E+3	5.98E+3	2.73E+7	1.64	3.61
T2A (120)	3.17E+3	2.47E+3	8.49E+6	1.28	3.73
T2B (120)	5.83E+3	4.51E+3	2.83E+7	1.29	2.06

RNA-transfected cells than in JFH-1 RNA-transfected cells; however, they were lower than in J6/JFH-1 RNA-transfected cells (Fig. 9C).

Transfected cells were serially passaged, and, importantly, both types of transfected cells (J6/JFH2/AS/mtT1A and J6/JFH2/AS/mtT1B RNA) secreted core protein and HCV RNA at high levels, even at the first passage after transfection, and the levels of HCV core protein and RNA were maintained during the passages (Fig. 10A and B). Infectious titers in the medium of the transfected cells were also measured (Fig. 10C). J6/JFH2/AS/mtT1A secreted a higher infectious titer than J6/JFH2/AS/mtT1B although their HCV core protein levels and RNA levels in the culture medium were similar. To confirm the rapid infectious viral production phenotype of these viruses, we inoculated naive Huh-7.5.1 cells with the culture medium of J6/JFH2/AS/mtT1A and J6/JFH2/AS/mtT1B RNA-transfected cells at 8 and 38 days posttransfection at an MOI of 0.01. All of the inoculated cells secreted core protein and HCV RNA with similar kinetics (Fig. 11A and B). The infectious titer was also determined in the culture medium of the infected and passaged cells (Fig. 11C). mtT1B (day 38 posttransfection) showed lower infectivity at 7 days after inoculation; however, substantial infectivity was detected at 13 and 27 days. The culture medium of mtT1A (day 8 and day 38 posttransfection) was harvested at 20 days after inoculation and analyzed by a sucrose density gradient assay, as described above (Fig. 11D). Major peaks of both HCV core protein and RNA were clearly shown at around 1.15 mg/ml, and the subpeaks of HCV core protein were found in lighter fractions. On the other hand, major peaks of infectivity were found at around 1.0 mg/ml. Compared to the data shown in Fig. 6E, the HCV core and RNA levels and infectivity titer are higher in mtT1A (day 8 and day 38 posttransfection) virus. The similar virus characteristics suggested that J6/JFH2/AS/mtT1A and J6/JFH2/AS/mtT1B viruses do not need further adaptations for autonomous expansion in cultured cells. Thus, we established stable cell culture-adapted virus and constructed recombinant cell culture-adapted infectious HCV clones by reverse genetics.

Human hepatocyte-transplanted uPA/SCID mouse experiment. To determine the *in vivo* infectivity of J6/JFH2/AS virus, we inoculated day 75 culture medium of T1B cells containing 1×10^6 RNA copies of purified J6/JFH2/AS HCV particles and original patient serum also containing 1×10^6 RNA copies into human hepatocyte-transplanted uPA/SCID mice. Inoculation of 1×10^6 RNA copies of cell culture-derived J6/JFH1 virus usually results in robust infection for human hepatocyte-transplanted uPA/SCID mice. Two mice were used for each type of inoculum. Human albumin levels in sera of the inoculated mice were more than 3 mg/ml during the experiment, which supported the high replacement ratio of the human hepatocytes in the mouse liver. Both mice inoculated with patient serum became HCV RNA positive 1 week postinoculation and remained positive during the 4-month observation period (Fig. 12). However, the mice inoculated with J6/JFH2/AS virus in culture medium did not become HCV positive after inoculation (Fig. 12). One mouse inoculated with J6/JFH2/AS virus died 16 days after inoculation, and the cause of death was unknown. HCV RNA was not detected at 7, 14, and 16 days postinoculation. The other mouse inoculated with culture medium was also tested every week for serum HCV RNA and remained negative for 56 days after infection. On day 56, this mouse received a second inoculation with the same culture medium. This mouse was monitored for a total of 63 days, but weekly tests for HCV RNA were continuously negative. Thus, the cell culture-adapted virus in the inoculum may be less viable *in vivo* although the virus acquired robust replication capacity in HuH-7 cells.

Full-length JFH-2 construct. We successfully established J6/JFH2/AS-derived cell culture-adapted viruses. Next, we produced a full-length JFH2/AS virus by using the structural region sequence from JFH-2. pJFH2/AS was constructed according to the viral sequence, and an alanine-to-serine mutation was introduced at amino acid position 2217. JFH2/AS RNA synthesized *in vitro* was electroporated into the Huh-7.5.1 cells, as described above. J6/JFH2/AS RNA was also transfected simultaneously and compared. Two groups of independently transfected cells (transfections 3 and 4 [T3 and T4, respectively]) were analyzed for JFH2/AS and J6/JFH2/AS. Interestingly, JFH2/AS RNA-transfected cells be-

cell lines were not tested (*). (D) The passaged transfected cells were stained with anti-core protein monoclonal antibody (2H9) as a primary antibody at the indicated time points. Green, HCV core protein; blue, 4′,6′-diamidino-2-phenylindole (DAPI) staining. (E) Density gradient analysis of culture supernatant from HCV RNA-transfected Huh-7.5.1 cells. Culture supernatants of transfected cell line T1A collected at 5 days, 8 weeks, and 11 weeks posttransfection were cleared by centrifugation and filtration. Each supernatant was overlaid on the stepwise sucrose density gradient (0%, 10%, 20%, 30%, 40%, 50%, and 60% sucrose) and centrifuged for 16 h at 200,000 × *g* at 4°C. Eighteen fractions were collected from the bottom of the tubes, and the concentration of HCV core protein in each fraction was determined by Lumipulse Ortho HCV Ag. The levels of HCV core protein, HCV RNA, and infectivity were determined in each fraction. Infectivity of the samples from day 5 was negative. Open diamond, buoyant density.

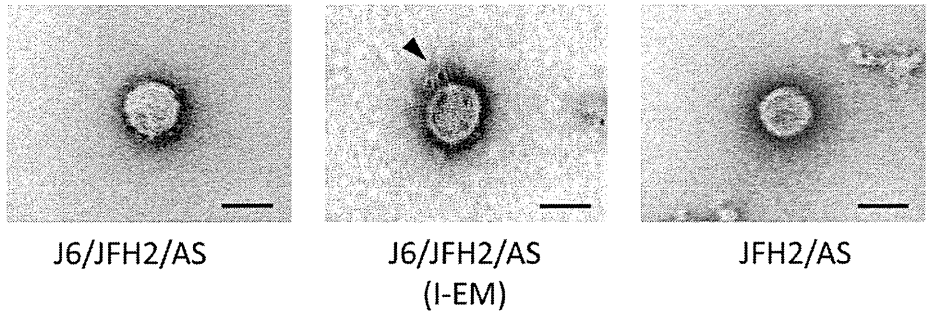

FIG 7 Morphology of JFH-2 virus particles. Negatively stained HCV particles were observed by electron microscopy. J6/JFH-2/AS and JFH2/AS virus particles were purified and observed by electron microscopy by using negative staining. In the middle panel, a J6/JFH-2/AS virus particle was detected by immuno-electron microscopic (I-EM) analysis by using anti-E2 antibody. Arrowhead, gold-labeled antibody. Scale bar, 50 nm.

gan to secrete core proteins earlier than J6/JFH2/AS RNA-transfected cells in this experiment (Fig. 13). Core protein levels were 24,525 and 11,720 fmol/liter in T3 cells at 67 days posttransfection and T4 cells at 63 days posttransfection, respectively. Infectious titers were also determined in the same culture medium at 2.1×10^4 and 4.3×10^4 focus-forming units (FFU)/ml for T3 and T4, respectively. T3 culture medium at day 67 posttransfection was

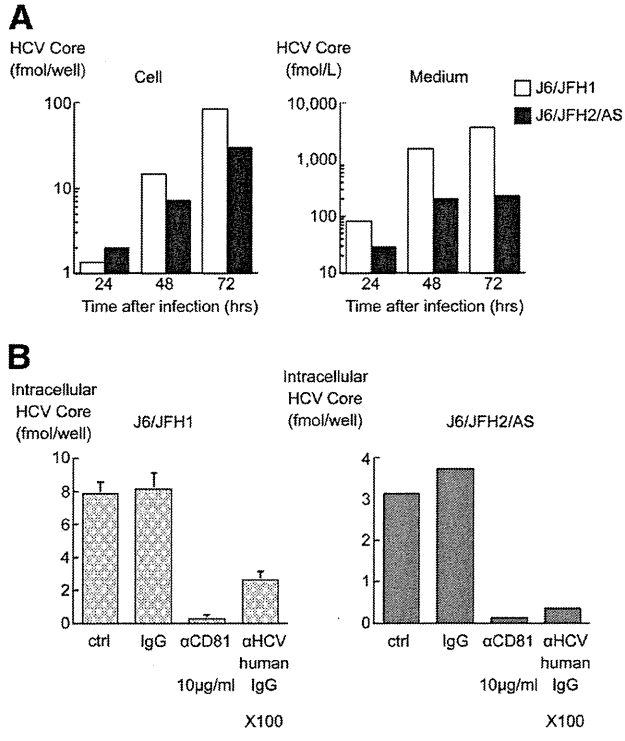

FIG 8 Comparative analysis between J6/JFH1 and J6/JFH2/AS virus. (A) Huh-7.5.1 cells were infected with J6/JFH1 or J6/JFH2/AS virus particles at an MOI of 0.03. HCV core protein production in the inoculated cell lysate and medium was measured at the indicated times. Assays were performed in duplicate, and the average data are represented. (B) Infection with J6/JFH1 and J6/JFH2/AS virus particles was inhibited by adding antibodies to the reaction mixtures. Assays were performed three times independently, and data are presented as means ± standard deviations. Normal human IgG and anti-CD81 monoclonal antibody and anti-HCV human IgG at the indicated concentrations were used. Ctrl, control.

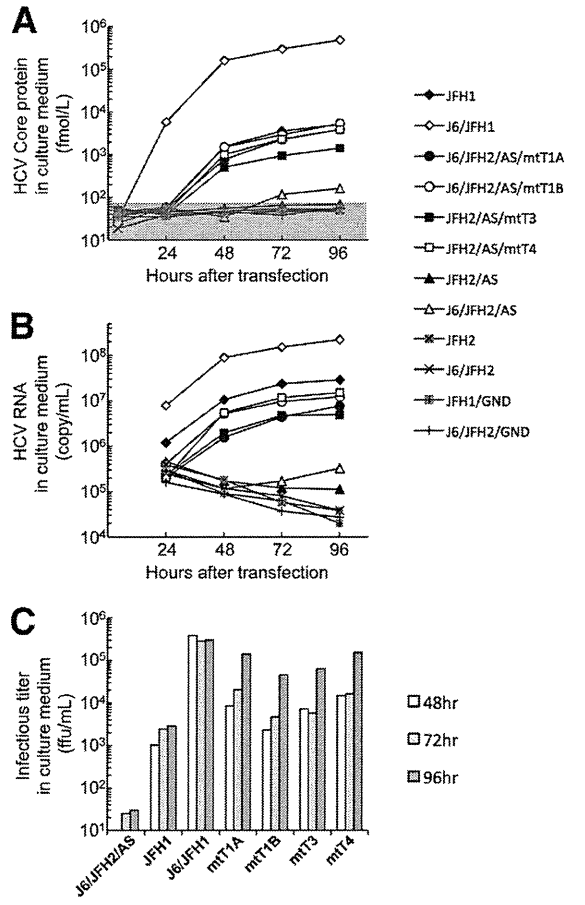

FIG 9 Transient virus production assay of J6/JFH2- and JFH2-related constructs with Huh-7.5.1 cells. Full-length HCV RNA was synthesized from the JFH1, J6/JFH1, JFH2, and J6/JFH2 constructs and their derivatives with mutations and transfected into Huh-7.5.1 cells. (A) HCV core protein levels in the culture medium were determined at 4, 24, 48, 72, and 96 h after transfection. The gray area indicates values that are below the detection limit. (B) HCV RNA levels in the culture medium were also determined at 24, 48, 72, and 96 h after transfection. (C) Infectivity in the culture medium was determined by focus formation assay at 48, 72, and 96 h after transfection. Only positively detected data are shown in the figure. All assays in this figure were performed in duplicate, and the average data are represented.

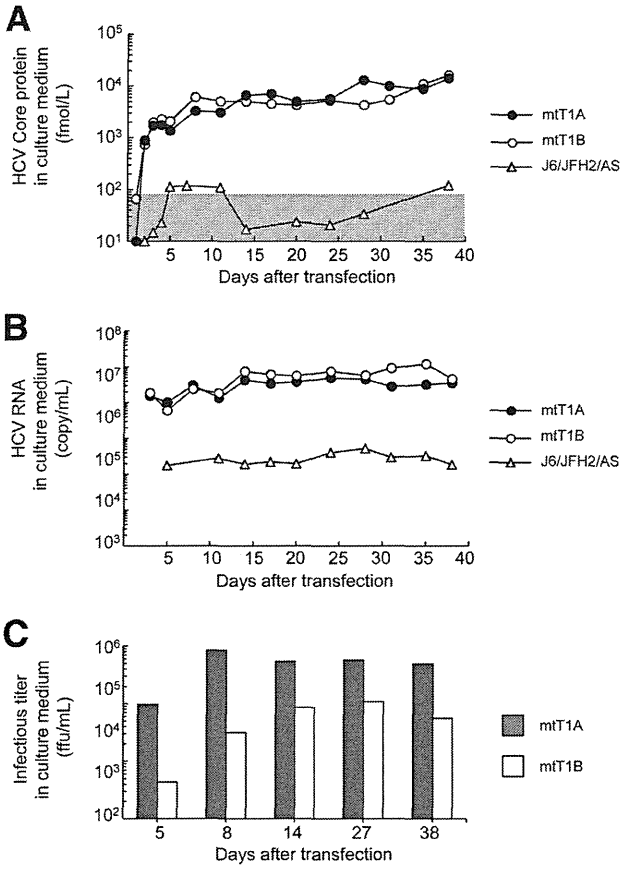

FIG 10 Continuous passage of J6/JFH2/AS cell culture-adapted virus RNA-transfected cells. Full-length HCV RNA was synthesized from the J6/JFH2/AS, J6/JFH2/AS/mtT1A (mtT1A), and J6/JFH2/AS/mtT1B (mtT1B) constructs. RNA-transfected cells were serially passaged until 38 days after transfection, and culture supernatants were harvested at the indicated time points. HCV core protein (A) and HCV RNA (B) levels in the culture media were determined. The data in the gray area were below the detection limit of the assay to detect HCV core protein. (C) Infectivity in the culture medium was determined by focus formation assay at 5, 8, 14, 27, and 38 days after transfection.

also used for electron microscopy analysis. After the density gradient purification, spherical viral particles were detected (Fig. 7, right panel). After the core protein levels plateaued, naive Huh-7.5.1 cells were inoculated with the culture medium, as described above. When the core protein levels plateaued again after the third inoculation of T3 and T4 cells, we sequenced the viral genome in the culture medium (T3i3 and T4i3, respectively) to determine the adaptive mutation. We found the following nonsynonymous mutations: 414IT in E2, 1510EG and 1617RQ in NS3, 2006KQ, 2233AV and 2234NS in NS5A, and 2695TI in NS5B of T3i3; and 387VG in E1, 828VA in NS2, 1225RQ and 1283RG in NS3, 1883VA in NS4B, 2206SA, 2279KN, and 2441CR in NS5A, and 2695TI in NS5B of T4i3 (Fig. 3B). We introduced these mutations into the pJFH2/AS plasmid (pJFH2/AS/mtT3 and pJFH2/AS/mtT4). Synthesized RNA from pJFH2/AS/mtT3 and pJFH2/AS/mtT4 and the related control plasmids was transfected into Huh-7.5.1 cells. HCV core protein levels, HCV RNA levels, and infectivity were monitored in the culture medium of the transfected cells until 96 h after transfection (Fig. 9A to C). JFH2/AS/mtT3 (mtT3) and JFH2/AS/mtT4 (mtT4) secreted similar levels of HCV core protein, RNA, and infectious virus with J6/JFH2/AS/mtT1A and J6/JFH2/AS/mtT1B. Although JFH2/AS/mtT3 secreted slightly higher levels of HCV core protein and RNA than JFH2/AS/mtT4, the secreted infectious virus titers were similar for both viruses. JFH2/AS/mtT3 and JFH2/AS/mtT4 RNA-transfected cells were also serially passaged, and the HCV core proteins were secreted immediately after transfection (Fig. 14A). However, JFH2 and JFH2/AS RNA-transfected cells did not secrete significant amounts of HCV core protein into the culture medium. HCV RNA levels in the culture medium of the RNA-transfected cells were at similar levels for JFH2/AS/mtT3 and JFH2/AS/mtT4 (around 10^7 copy/ml) (Fig. 14B). Infectivity was also detected as higher than 10^4 FFU/ml even at 3 days after the RNA transfection, and this level of infectious titer was maintained during the cell passages (Fig. 14C). We also analyzed JFH2/AS/mtT3 and JFH2/AS/mtT4 culture media by density gradient assay (Fig. 14D). The density profiles with HCV core protein and RNA levels and infectious titers in the fractions were basically similar to those of J6/JFH2/AS-adapted viruses (Fig. 6E and 11D). Taken together, the results described in this section indicate infectious virus was also recovered from the full-length JFH-2 construct with the 2217AS mutation.

Mechanistic analysis of adaptive mutations introduced in the J6/JFH2/AS and JFH2/AS cell culture-adapted viruses. To elucidate the mechanisms of adaptive mutations discovered in J6/JFH2/AS and JFH2/AS virus genomes, we transfected JFH-2 and J6/JFH2 constructs along with possible control constructs into Huh7-25 cells (2) (Fig. 15), which are CD81 defective. The transfection of JFH-1 RNA into Huh7-25 cells results in infectious HCV production, but there was no reinfection into Huh7-25 cells because the cell surface expression of CD81 is essential for HCV infection (10). HCV core protein levels were measured in the culture medium and cell lysate to monitor virus particle secretion and intracellular virus genome replication, respectively (Fig. 15A and B). JFH2/AS, JFH2, J6/JFH2, JFH1/GND, and J6/JFH2/GND RNA-transfected cells did not show increased levels of intracellular core protein expression. However, other RNA-transfected cells showed increased intracellular core protein expression. The cellular core protein level was especially increased at 72 and 96 h after transfection with J6/JFH2/AS RNA, which suggests a higher replication efficiency than J6/JFH; however, core protein secretion was not detected with J6/JFH2/AS, which suggests defective virus particle formation or secretion. Other adaptive mutations in J6/JFH2/AS/mtT1A and J6/JFH2/AS/mtT1B further increased virus genome replication and core protein secretion. In the case of JFH2/AS RNA transfection, cellular core protein expression was not detected, suggesting a lower replication efficiency than that of J6/JFH2/AS. This lower replication efficiency of JFH2/AS may be due to the presence of different sequences in the region of core protein to NS2. However, core protein expression in the cell lysate and culture medium was detected with both JFH2/AS/mtT3 and JFH2/AS/mtT4 RNA transfection. Thus, adaptive mutations in mtT3 and mtT4 are necessary to increase viral genome replication and efficient core protein secretion. JFH-1 and J6/JFH-1 had intracellular core protein expression levels that were similar and high. From the intracellular core protein data, it is clear that J6/JFH2/AS/mtT1A, J6/JFH2/AS/mtT1B, JFH2/AS/mtT3, and JFH2/AS/mtT4 constructs obtained higher replication capacities by

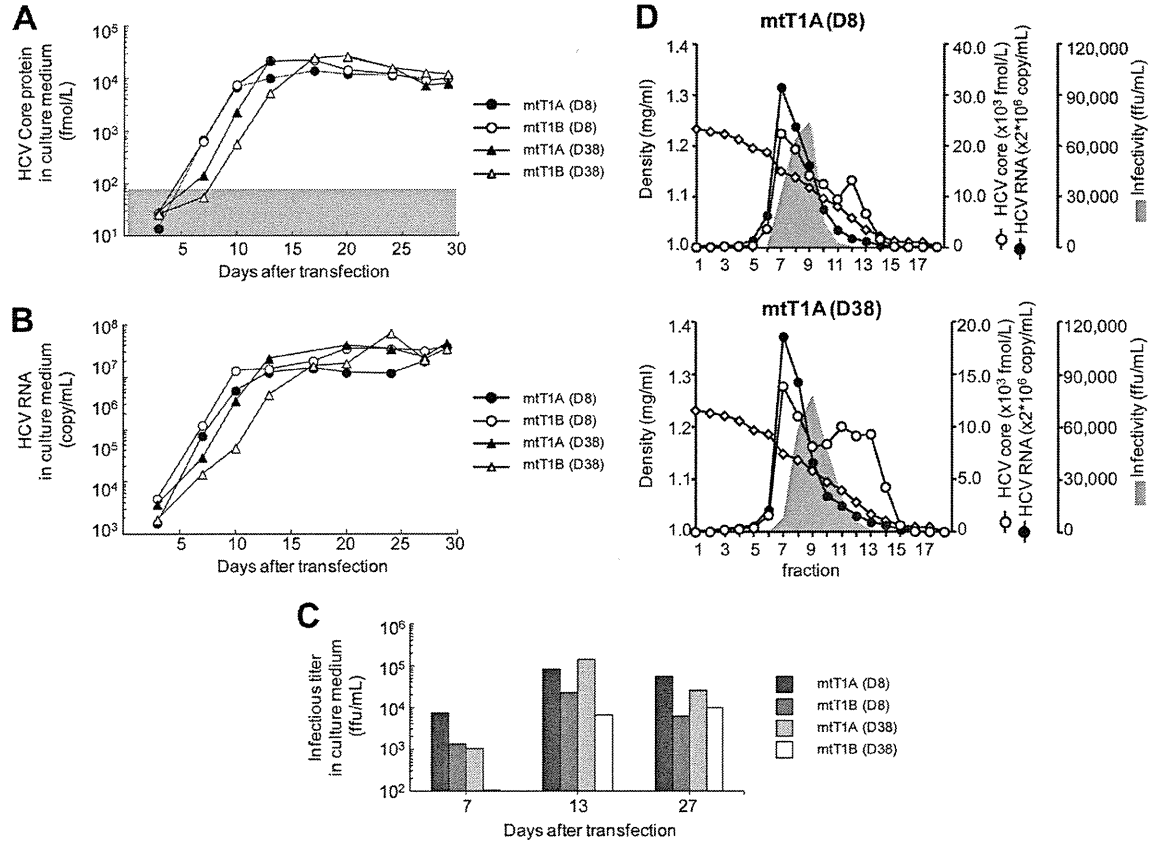

FIG 11 Serial passages of J6/JFH2/AS cell culture-adapted virus infected cells. Naive Huh-7.5.1 cells were inoculated with culture medium of the RNA-transfected cells at an MOI of 0.01. Inoculated cells were serially passaged, and culture supernatants were harvested at the indicated times. HCV core protein (A), HCV RNA (B), and infectivity (C) levels in the culture media were determined. (D) Density gradient analysis of culture supernatant from J6/JFH2/AS/mtT1A cell-culture adapted virus-infected Huh-7.5.1 cells. Culture supernatant of infected Huh-7.5.1 cells with mtT1A (day 8 [D8] D38 posttransfection) was harvested at 20 days after inoculation. Assays were performed as described in the legend of Fig. 6E. Open diamond, buoyant density.

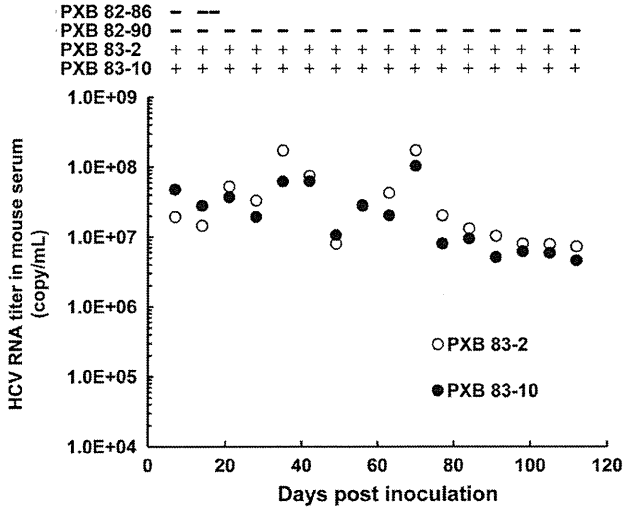

FIG 12 Serum HCV RNA titer in human hepatocyte-transplanted uPA/SCID mice inoculated with JFH-2 serum and cell culture-adapted virus. Mice PXB 82-86 and PXB 82-90 were inoculated with the cell culture-adapted J6/JFH2/AS HCV particles, and mice PXB 83-2 and PXB 83-10 were inoculated with JFH-2 patient serum. Upper and lower panels indicate the results of the RT-PCR and the quantitative detection RT-PCR of HCV RNA in mouse serum, respectively.

adaptive mutations; however, their replication levels are lower than those of JFH-1 and J6/JFH1.

We also analyzed the ratio of extracellular protein to total core protein to analyze the virus secretion efficiency (Fig. 15C). J6/JFH-1 secreted a higher percentage of core protein into culture

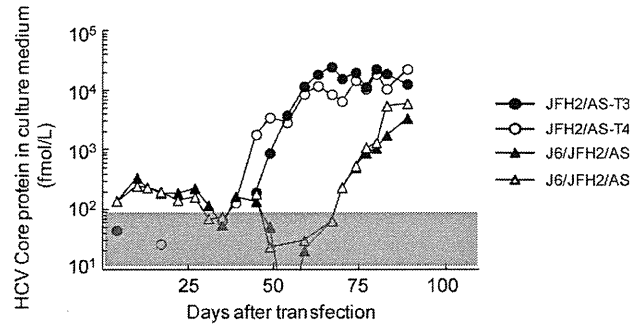

FIG 13 Propagation of a full-length JFH2 virus. Huh-7.5.1 cells were transfected with the transcribed RNA from pJFH2/AS and pJ6/JFH2/AS. Two independently JFH2/AS RNA-transfected cell lines (T3 and T4) were independently passaged. At each time point, culture medium was harvested and analyzed for the presence of HCV core protein.

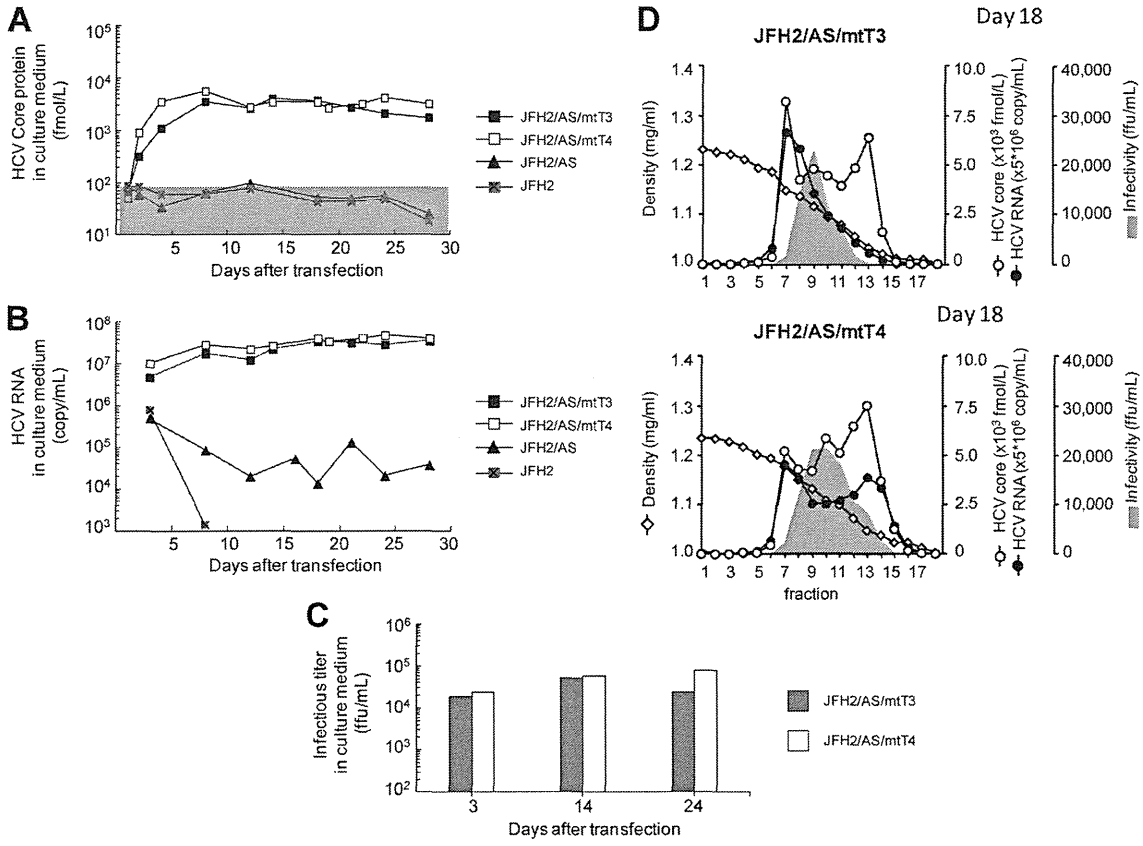

FIG 14 Full-length RNA was synthesized from the JFH2 construct and its derivatives with mutations. RNA-transfected cells were serially passaged, and culture supernatants were harvested at the indicated time points. HCV core protein (A), HCV RNA (B), and infectivity (C) levels in the culture media were determined. The data in the gray area were below the detection limit of the assay to detect HCV core protein. (D) Density gradient analysis of culture supernatant from JFH2/AS cell-culture adapted virus-infected Huh-7.5.1 cells. Culture supernatants of Huh-7.5.1 cells infected with JFH2/mtT3 and JFH2/mtT4 viruses were harvested 18 days after inoculation. Assays were performed as described in the legend of Fig. 6E. Open diamond, buoyant density.

medium than JFH-1. J6/JFH2/AS/mtT1A, J6/JFH2/AS/mtT1B, JFH2/AS/mtT3, and JFH2/AS/mtT4 RNA-transfected cells showed different percentages of secreted core protein. mtT1A and mtT1B constructs showed similar replication levels (Fig. 15B), but mtT1B showed a higher percentage of core protein secretion than mtT1A (Fig. 15C). mtT3 and mtT4 showed similar percentages of core protein secretion, which are higher than the level of JFH1 (Fig. 15C). Because J6/JFH2/AS RNA-transfected cells did not secrete core protein despite intracellular core protein expression (Fig. 15A and B), the adaptive mutant constructs obtained core protein (or virus particle) secretion phenotypes. Thus, during the adaptation process, the viruses obtained both higher replication capacity and core protein secretion capacity by their adaptive mutations.

Other HCV constructs with the 2217AS mutation. The alanine residue at amino acid position 2217 is located in the ISDR of NS5A, and it is conserved among HCV strains including genotype 1 and 2 strains. Because the 2217AS mutation in NS5A is the key mutation for the production of cell culture-adapted HCV, we introduced this mutation into other wild-type HCV constructs, i.e., H77 (genotype 1a), Con1 (genotype 1b), and J6CF (genotype 2a). Synthetic RNAs including the 2217AS mutation were electroporated into Huh-7.5.1 cells, and then the transfected cells were serially passaged. HCV core protein secretion was measured in the culture medium of transfected cells. However, we could not observe the increment of HCV core levels in the culture medium (data not shown). Therefore, we concluded that the 2217AS mutation does not always induce cell culture adaptation in HCV isolates.

DISCUSSION

In previous studies, we have isolated cell culture-infectious HCV, the JFH-1 strain, from a patient with fulminant hepatitis (14, 38). In this report, we isolated another HCV cDNA, named JFH-2, also from a fulminant hepatitis patient. We constructed a subgenomic replicon with the JFH-2 sequence, but its replication efficiency was low. Among the mutations found in the replicon genome, the 2217AS mutation in the ISDR exhibited the strongest adaptive effect. Interestingly, the full-length chimeric or wild-type JFH-2 genome with adaptive mutations could replicate and produce infectious virus particles. Virus infection efficiency was sufficient for autonomous virus propagation in cultured cells.

Several full-length HCV cDNAs have been cloned, and their infectivity has been confirmed *in vivo* with chimpanzee models (18, 39). However, it has been difficult to produce recombinant viral particles and test their infectivity by using cell culture

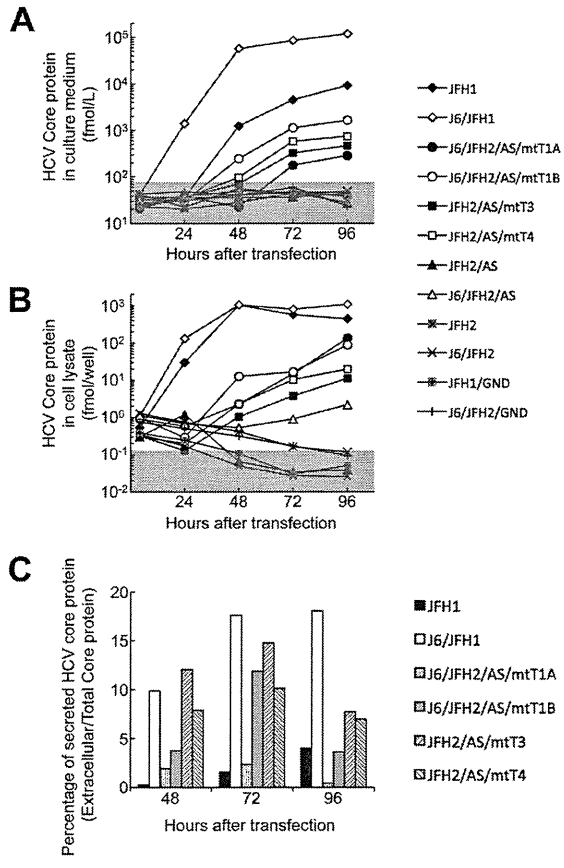

FIG 15 Transient virus production assay of J6/JFH2- and JFH2-related constructs with CD81-defective Huh7-25 cells. Full-length HCV RNA was synthesized from the JFH1, J6/JFH1, JFH2, and J6/JFH2 constructs and their derivatives with mutations and transfected into Huh7-25 cells. (A) HCV core protein levels in culture medium were determined at 4, 24, 48, 72, and 96 h after transfection. The data in the gray area were below detection limit. (B) HCV core protein levels in the cell lysate were determined at 24, 48, 72, and 96 h after transfection. (C) Percentages of secreted HCV core protein from the transfected cells were determined at 48, 72, and 96 h after transfection. Percentages of secreted HCV core protein were calculated only for the indicated viruses. All assays were performed in duplicate, and the data represent average values.

systems (4, 28). Only the JFH-1 strain efficiently replicates in HuH-7 cells and other hepatic and nonhepatic cell lines in subgenomic replicon form (20, 38, 41). Full-length wild-type JFH-1 RNA and chimeric JFH-1 RNA can replicate in HuH-7 cells and produce infectious virus. Since the JFH-1 strain was isolated from a patient with fulminant hepatitis, we assumed that virus strains that cause fulminant hepatitis may replicate efficiently in cultured cells. To identify more HCV clones that can replicate in cultured cells, we isolated the JFH-2 strain from another fulminant hepatitis patient (15). Interestingly, the JFH-2 strain showed a low level of replication in cultured cells in the initial subgenomic replicon experiment. This result may suggest that HCV strains isolated from fulminant hepatitis patients are able to replicate more efficiently than strains from chronic hepatitis patients; however, this hypothesis should be confirmed by testing more HCV strains from patients with fulminant hepatitis. The JFH-2 patient received a course of betamethasone therapy and developed fulminant hepatitis after the withdrawal of betamethasone. It is thus possible that the JFH-2 strain obtained its higher replication capacity in the immune-suppressed host environment. To confirm this hypothesis, we must test the replication efficiency of HCV strains isolated from other immune-suppressed patients, such as patients who are coinfected with HIV, patients who are reinfected after a transplant, and patients who are treated with immunosuppressive agents.

In previous reports, adaptive mutations have been found to enhance viral RNA replication at the expense of virus particle formation efficiency (28). A highly cell culture-adapted Con1 strain can replicate in cultured cells, but it cannot produce infectious virus particles. Interestingly, a highly adapted Con1 strain was not infectious for chimpanzees, while moderately adapted Con1 was infectious. However, the virus recovered from the infected animal was wild-type Con1 virus (5). This result clearly suggests that HCV strains with lower replication efficiencies are favorable for *in vivo* infection. However, we must note that the "replication efficiency" is determined in cultured cells. In the case of JFH-2, we found several adaptive mutations in the subgenomic replicon clones, and the most adaptive mutation, 2217AS, was tested in full-length HCV replication and virus production. After the RNA transfection of J6/JFH2/AS, we could not detect substantial virus secretion for about 30 days. However, after 30 days, significant levels of infectious virus particles were secreted into the culture medium. Naive Huh-7.5.1 cells were inoculated three times with the cell culture-adapted virus. This virus adaptation was also tested with full-length JFH2/AS, and we successfully obtained infectious JFH2/AS virus. Both the J6/JFH2/AS and JFH2/AS viruses acquired the ability for autonomous virus expansion in Huh-7.5.1 cells, and several additional mutations were found in their genomes. Interestingly, the 2695TI mutation in NS5B was commonly found in all of the adapted virus genomes, and isoleucine at amino acid position 2695 is also found in the JFH-1 strain. However, the introduction of only the 2695TI mutation into the J6/JFH2/AS or JFH2/AS virus genome did not restore robust virus production (data not shown). After repeated virus passages, mutations were found throughout the viral genome (in J6/JFH2/AS-T1Ai3 and -T1Bi3 and in JFH2/AS-T3i3 and -T4i3), and we are currently investigating which mutations or combinations of mutations are most important for this adaptation. From the comparisons of cell culture-adapted viruses and their parental virus constructs, adaptive mutations are necessary to increase both viral genome replication and virus particle assembly/secretion efficiency (Fig. 15). The procedure to produce cell culture-adapted HCV was thus established. The adaptive mutations found from the subgenomic replicon assay were introduced into the full-length genome, and the cells transfected with virus RNA were repeatedly passaged until the virus particles were produced.

In vivo infectivity may be inversely related to the replication efficiency in cultured cells, as discussed above. The original JFH-2 patient serum was infectious in human liver-transplanted mice; however, cell culture-adapted J6/JFH2/AS virus was not infectious. The JFH-1 virus was infectious not only for cultured cells but also for chimpanzees and human liver-transplanted mice (10, 38). However, the JFH-1 infection in chimpanzees was only mild and transient without any liver pathology. Thus, the J6/JFH2/AS and JFH2/AS viruses are more cell culture-adapted and attenuated than the JFH-1 virus. It may be worthwhile to test this cell culture-

adapted strain as a live attenuated vaccine candidate to induce protective immunity. However, for ethical reasons, the necessary chimpanzee experiments are not appropriate to perform. Therefore, we should wait for the establishment of immunocompetent small-animal models susceptible to HCV infection to perform this kind of study. Furthermore, future studies should examine the *in vivo* infectivity of the adapted J6/JFH2 and JFH2 viruses isolated in the present study.

The 2217AS mutation is located in the ISDR. In the previous study of the genotype 1b subgenomic replicon, mutations introduced into the ISDR enhanced the colony formation efficiency of the HCV replicons (17, 23). However, mutations in the ISDR impaired the genotype 1b HCV replication in human liver-transplanted mice (9). The exact mechanism of the ISDR is still not clear although the number of mutations in the ISDR is related to the efficacy of interferon therapy (8). Our results in this study also support the concept that the 2217AS mutation in the ISDR enhances replicon replication efficiency although the J6/JFH2/AS virus did not infect human liver-transplanted mice. Further studies are necessary to understand the molecular mechanism of the effects of adaptive mutations in the ISDR.

In the present study, we established a cell culture-adapted HCV strain, JFH-2. The virus could be passaged continuously in naive Huh-7.5.1 cells. This approach may be applicable to the establishment of new infectious HCV clones. Novel antiviral drugs are under development, and some of them will be used in the clinical setting. However, most of them target genotype 1 HCV strains. To eradicate other genotypes of HCV, it is important to establish their replicons and infectious virus culture systems.

ACKNOWLEDGMENTS

Huh-7.5.1 cells were kindly provided by Francis V. Chisari. The J6CF plasmid was a kind gift from Jens Bukh. Anti-HCV human IgG was a kind gift from Hiroshi Yoshizawa and Junko Tanaka, Hiroshima University. AP33 antibody was generously provided by Genentec. We thank Tetsuro Suzuki and Hideki Aizaki for their helpful discussions. We also thank Minako Kaga for her technical assistance.

This work was partially supported by Grants-in-Aid for Scientific Research from the Japan Society for the Promotion of Science, from the Ministry of Health, Labor and Welfare of Japan, from the Ministry of Education, Culture, Sports, Science and Technology, from the National Institute of Biomedical Innovation, and by the Research on Health Sciences Focusing on Drug Innovation from the Japan Health Sciences Foundation.

REFERENCES

1. **Aizaki H, et al.** 2008. Critical role of virion-associated cholesterol and sphingolipid in hepatitis C virus infection. J. Virol. **82**:5715–5724.
2. **Akazawa D, et al.** 2007. CD81 expression is important for the permissiveness of Huh7 cell clones for heterogeneous hepatitis C virus infection. J. Virol. **81**:5036–5045.
3. **Akazawa D, et al.** 2011. Production and characterization of HCV particles from serum-free culture. Vaccine **29**:4821–4828.
4. **Bartenschlager R, Lohmann V.** 2000. Replication of hepatitis C virus. J. Gen. Virol. **81**:1631–1648.
5. **Bukh J, et al.** 2002. Mutations that permit efficient replication of hepatitis C virus RNA in Huh-7 cells prevent productive replication in chimpanzees. Proc. Natl. Acad. Sci. U. S. A. **99**:14416–14421.
6. **Choo QL, et al.** 1989. Isolation of a cDNA clone derived from a blood-borne non-A non-B viral hepatitis genome. Science **244**:359–362.
7. **Di Bisceglie AM, Hoofnagle JH.** 2002. Optimal therapy of hepatitis C. Hepatology **36**:S121–S127.
8. **Enomoto N, et al.** 1995. Sensitivity to interferon is conferred by amino acid substitutions in the NS5A region. J. Clin. Invest. **96**:224–230.
9. **Hiraga N, et al.** 2011. Impact of viral amino acid substitutions and host interleukin-28b polymorphism on replication and susceptibility to interferon of hepatitis C virus. Hepatology **54**:764–771.
10. **Kato T, et al.** 2008. Hepatitis C virus JFH-1 strain infection in chimpanzees is associated with low pathogenicity and emergence of an adaptive mutation. Hepatology **48**:732–740.
11. **Kato T, et al.** 2003. Efficient replication of the genotype 2a hepatitis C virus subgenomic replicon. Gastroenterology **125**:1808–1817.
12. **Kato T, et al.** 2005. Detection of anti-hepatitis C virus effects of interferon and ribavirin by a sensitive replicon system. J. Clin. Microbiol. **43**:5679–5684.
13. **Kato T, et al.** 2006. Cell culture and infection system for hepatitis C virus. Nat. Protoc. **1**:2334–2339.
14. **Kato T, et al.** 2001. Sequence analysis of hepatitis C virus isolated from a fulminant hepatitis patient. J. Med. Virol. **64**:334–339.
15. **Kato T, et al.** 2003. Processing of hepatitis C virus core protein is regulated by its C-terminal sequence. J. Med. Virol. **69**:357–366.
16. **Kiyosawa K, et al.** 1990. Interrelationship of blood transfusion, non-A, non-B hepatitis and hepatocellular carcinoma: analysis by detection of antibody to hepatitis C virus. Hepatology **12**:671–675.
17. **Kohashi T, et al.** 2006. Site-specific mutation of the interferon sensitivity-determining region (ISDR) modulates hepatitis C virus replication. J. Viral Hepat. **13**:582–590.
18. **Kolykhalov AA, et al.** 1997. Transmission of hepatitis C by intrahepatic inoculation with transcribed RNA. Science **277**:570–574.
19. **Kuo G, et al.** 1989. An assay for circulating antibodies to a major etiologic virus of human non-A non-B hepatitis. Science **244**:362–364.
20. **Lindenbach BD, et al.** 2005. Complete replication of hepatitis C virus in cell culture. Science **309**:623–626.
21. **Lindenbach BD, et al.** 2006. Cell culture-grown hepatitis C virus is infectious in vivo and can be recultured in vitro. Proc. Natl. Acad. Sci. U. S. A. **103**:3805–3809.
22. **Lohmann V, et al.** 1999. Replication of subgenomic hepatitis C virus RNAs in a hepatoma cell line. Science **285**:110–113.
23. **Maekawa S, et al.** 2004. Introduction of NS5A mutations enables subgenomic HCV replicon derived from chimpanzee-infectious HC-J4 isolate to replicate efficiently in Huh-7 cells. J. Viral Hepat. **11**:394–403.
24. **McHutchison JG, et al.** 1998. Interferon alfa-2b alone or in combination with ribavirin as initial treatment for chronic hepatitis C. N. Engl. J. Med. **339**:1485–1492.
25. **Merck & Co.** 2011. Victrelis (boceprevir) prescribing information. Merck & Co., Whitehouse Station, NJ. http://www.accessdata.fda.gov/drugsatfda_docs/label/2011/202258lbl.pdf.
26. **Murayama A, et al.** 2007. The NS3 helicase and NS5B-to-3′X regions are important for efficient hepatitis C virus strain JFH-1 replication in Huh7 cells. J. Virol. **81**:8030–8040.
27. **Murayama A, et al.** 2010. RNA polymerase activity and specific RNA structure are required for efficient HCV replication in cultured cells. PLoS Pathog. **6**:e1000885. doi:10.1371/journal.ppat.1000885.
28. **Pietschmann T, et al.** 2002. Persistent and transient replication of full-length hepatitis C virus genomes in cell culture. J. Virol. **76**:4008–4021.
29. **Pietschmann T, et al.** 2009. Production of infectious genotype 1b virus particles in cell culture and impairment by replication enhancing mutations. PLoS Pathog. **5**:e1000475. doi:10.1371/journal.ppat.1000475.
30. **Poynard T, et al.** 1998. Randomised trial of interferon α2b plus ribavirin for 48 weeks or for 24 weeks versus interferon α2b plus placebo for 48 weeks for treatment of chronic infection with hepatitis C virus. Lancet **352**:1426–1432.
31. **Saeed M, et al.** 2009. Evaluation of hepatitis C virus core antigen assays in detecting recombinant viral antigens of various genotypes. J. Clin. Microbiol. **47**:4141–4143.
32. **Takahashi H, et al.** 2010. Biological properties of purified recombinant HCV particles with an epitope-tagged envelope. Biochem. Biophys. Res. Commun. **395**:565–571.
33. **Tateno C, et al.** 2004. Near completely humanized liver in mice shows human-type metabolic responses to drugs. Am. J. Pathol. **165**:901–912.
34. **U. S. Food and Drug Administration.** 2011. FDA news release. FDA approves Incivek for hepatitis C. U.S. Food and Drug Administration, Silver Spring, MD. http://www.fda.gov/NewsEvents/Newsroom/PressAnnouncements/ucm256299.htm.
35. **U. S. Food and Drug Administration.** 2011. FDA news release. FDA approves Victrelis for hepatitis C. U.S. Food and Drug Administration,

Silver Spring, MD. http://www.fda.gov/NewsEvents/Newsroom/PressAnnouncements/ucm255390.htm.
36. **Vertex Pharmaceuticals.** 2011. Incivek (telaprevir) prescribing information. Vertex Pharmaceuticals, Cambridge, MA. http://www.accessdata.fda.gov/drugsatfda_docs/label/2011/201917lbl.pdf.
37. **Wakita T.** 2009. Isolation of JFH-1 strain and development of an HCV infection system. Methods Mol. Biol. **510**:305–327.
38. **Wakita T, et al.** 2005. Production of infectious hepatitis C virus in tissue culture from a cloned viral genome. Nat. Med. **11**:791–796.
39. **Yanagi M, Purcell RH, Emerson SU, Bukh J.** 1997. Transcripts from a single full-length cDNA clone of hepatitis C virus are infectious when directly transfected into the liver of a chimpanzee. Proc. Natl. Acad. Sci. U. S. A. **94**:8738–8743.
40. **Yanagi M, Purcell RH, Emerson SU, Bukh J.** 1999. Hepatitis C virus: an infectious molecular clone of a second major genotype (2a) and lack of viability of intertypic 1a and 2a chimeras. Virology **262**:250–263.
41. **Zhong JP, et al.** 2005. Robust hepatitis C virus infection in vitro. Proc. Natl. Acad. Sci. U. S. A. **102**:9294–9299.

JCM
Journals.ASM.org

Japanese Reference Panel of Blood Specimens for Evaluation of Hepatitis C Virus RNA and Core Antigen Quantitative Assays

Asako Murayama,[a] Nao Sugiyama,[a] Koichi Watashi,[a] Takahiro Masaki,[a] Ryosuke Suzuki,[a] Hideki Aizaki,[a] Toshiaki Mizuochi,[b] Takaji Wakita,[a] and Takanobu Kato[a]

Department of Virology II, National Institute of Infectious Diseases, Tokyo, Japan,[a] and Department of Research on Blood and Biological Products, National Institute of Infectious Diseases, Tokyo, Japan[b]

An accurate and reliable quantitative assay for hepatitis C virus (HCV) is essential for measuring viral propagation and the efficacy of antiviral therapy. There is a growing need for domestic reference panels for evaluation of clinical assay kits because the performance of these kits may vary with region-specific genotypes or polymorphisms. In this study, we established a reference panel by selecting 80 donated blood specimens in Japan that tested positive for HCV. Using this panel, we quantified HCV viral loads using two HCV RNA kits and five core antigen (Ag) kits currently available in Japan. The data from the two HCV RNA assay kits showed excellent correlation. All RNA titers were distributed evenly across a range from 3 to 7 log IU/ml. Although the data from the five core Ag kits also correlated with RNA titers, the sensitivities of individual kits were not sufficient to quantify viral load in all samples. As calculated by the correlation with RNA titers, the theoretical lower limits of detection by these core Ag assays were higher than those for the detection of RNA. Moreover, in several samples in our panel, core Ag levels were underestimated compared to RNA titers. Sequence analysis in the HCV core region suggested that polymorphisms at amino acids 47 to 49 of the core Ag were responsible for this underestimation. The panel established in this study will be useful for estimating the quality of currently available and upcoming HCV assay kits; such quality control is essential for clinical usage of these kits.

Hepatitis C virus (HCV) is a major cause of chronic liver disease worldwide (15). There is no protective vaccine against this virus, and once an individual is infected, HCV often establishes persistent infection and leads to chronic hepatitis, cirrhosis, and hepatocellular carcinoma (9). The most widely used therapy for HCV infection is the combined administration of pegylated alpha interferon and ribavirin (29). However, this treatment is problematic, as it has limited efficacy, high cost, and severe adverse effects (8, 25). To estimate the outcome of antiviral therapy, and to understand the state of viral propagation, it is important to determine the HCV viral load in chronic hepatitis C patients by the use of accurate and reliable HCV quantitative assays (9, 14). For this purpose, several commercial assay kits for HCV RNA and core antigen (Ag) quantification are currently used in Japan. For quantification of HCV RNA levels, two real-time quantitative reverse transcription-PCR (qRT-PCR)-based assay kits are available, including the COBAS AmpliPrep/COBAS TaqMan HCV test (CAP/CTM-RNA; Roche Diagnostics, Tokyo, Japan) and the Abbott RealTime HCV test (ART-RNA; Abbott Japan, Tokyo, Japan). These assays are known to have high sensitivity and a wide dynamic range, but they require technical skill and attention to maintaining the specified conditions (4–6, 16, 24, 33–35). Alternatively, HCV viremia can be quantified by assessment of HCV core Ag level (1–3, 7, 10, 12, 13, 17–22, 27, 30–32). Five HCV core Ag assay kits are commercially available in Japan, including Architect HCV Ag (Architect-Ag; Abbott Japan), Lumipulse Ortho HCV Ag (Lumipulse-Ag; Fujirebio, Tokyo, Japan), Lumispot Eiken HCV Ag (Lumispot-Ag; Eiken Chemical, Tokyo, Japan), the Ortho HCV Ag ELISA test (ELISA-Ag; Ortho Clinical Diagnostics, Tokyo, Japan), and the Ortho HCV Ag IRMA test (IRMA-Ag; Ortho Clinical Diagnostics, Tokyo, Japan). These assays have some disadvantages compared to those measuring HCV RNA (notably, low sensitivity and narrow range of quantification) but also have some advantages (including ease of use, reduced risk of contamination, reduced cost, and reliability even with samples stored at room temperature for extended periods of time [1, 32]). Although core Ag levels are thought to be related closely to HCV RNA titers, the correlation and linearity of core Ag levels have not yet been fully evaluated. In addition, these quantitative parameters are known to be affected by nucleotide and amino acid sequences at the target regions of the assays (5, 6, 28, 34), and this sequence variation depends on genotypes or predominant strains in specific geographical regions.

In this study, we established a Japanese reference panel of samples for evaluation of HCV RNA and core Ag levels by collecting donated blood specimens that tested positive for HCV RNA and anti-HCV antibodies. Using this reference panel, we evaluated the HCV loads in these specimens with two HCV RNA assay kits and five core Ag assay kits and assessed correlations among the data generated by these kits.

MATERIALS AND METHODS

Preparation of reference panel. To establish a reference panel for HCV quantitative assays, a total of 80 donated plasma samples were selected. All of these specimens, supplied by the Japanese Red Cross Blood Centers, tested positive for the presence of HCV RNA and anti-HCV antibodies. These samples, collected in Japan from May to September of 2007, were obtained from Japanese blood donor volunteers in various regions of

Received 20 February 2012 **Returned for modification** 21 March 2012
Accepted 30 March 2012
Published ahead of print 11 April 2012
Address correspondence to Takanobu Kato, takato@nih.go.jp.
Supplemental material for this article may be found at http://jcm.asm.org/.

doi:10.1128/JCM.00487-12

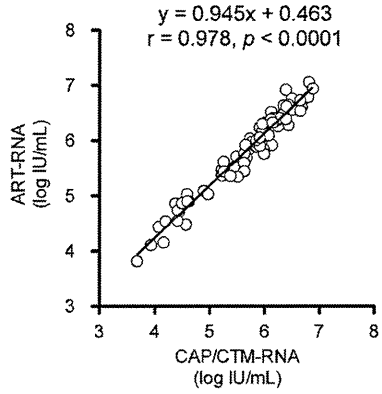

FIG 1 Correlation of HCV RNA titers as quantified by two commercial kits.

Japan. The samples were divided into 1-ml aliquots and stored at −80°C until use.

Quantification of HCV RNA and core Ag. The HCV RNA titer was measured with two real-time qRT-PCR kits, CAP/CTM-RNA (detection range, 1.5×10^1 to 6.9×10^7 IU/ml) and ART-RNA (detection range, 1.2×10^1 to 1.0×10^8 IU/ml). Additionally, samples were assessed using five HCV core Ag assay kits, including Architect-Ag (detection range, 3 to 20,000 fmol/liter), Lumipulse-Ag (detection range, 50 to 50,000 fmol/liter), Lumispot-Ag (detection range, 20 to 400,000 fmol/liter), ELISA-Ag (detection range, 44.4 to 3,600 fmol/liter), and IRMA-Ag (detection range, 20 to 20,000 fmol/liter). All assays were performed by the respective manufacturers at their research laboratories.

Sequencing and genotyping of HCV in reference panel samples. Viral RNA was extracted with the QIAamp viral RNA kit (Qiagen, Valencia, CA) from 140 μl of each plasma sample. HCV RNA was amplified by RT-PCR with primers corresponding to the 5′ untranslated region (UTR) (43S-IH, 5′-CCTGTGAGGAACTACTGTCTTC-3′; c/s17-ssp, 5′-CCGGGAGAGCCATAGTGGTCTGCG-3′) and the E1 region (1323R-IH, 5′-GGCGACCAGTTCATCATCAT-3′); the amplified products were sequenced directly. HCV genotypes of the isolated strains were assigned by phylogenetic analysis using an alignment with a representative strain of each genotype.

Statistical analysis. The correlations of obtained quantitative data were assessed by Pearson's correlation coefficient analysis, and values for r and P were calculated. A P value of <0.05 was considered to indicate statistical significance. Analysis was performed using Prism 5 software (GraphPad Software, Inc., La Jolla, CA).

Nucleotide sequence accession numbers. The accession numbers of C-01 to C-80 are AB705312 to AB705391, respectively.

RESULTS

Quantification of HCV RNA levels. The reference panel established in this work was used to measure HCV RNA levels with the CAP/CTM-RNA and ART-RNA kits. The correlation of the data obtained with the two kits is shown in Fig. 1. The RNA titers of these samples were distributed evenly, and all values were within the dynamic ranges of both assays. The HCV titers ranged from 3.68 to 6.88 and 3.82 to 7.08 log IU/ml in CAP/CTM-RNA and ART-RNA, respectively, and the correlation was significant ($r = 0.978$; $P < 0.0001$).

Quantification of HCV core Ag levels. HCV core Ag levels were measured using Architect-Ag, Lumipulse-Ag, Lumispot-Ag, ELISA-Ag, and IRMA-Ag kits. Among the 80 specimens in the reference panel, core Ag levels could be measured in all samples using Architect-Ag and ELISA-Ag kits, whereas core Ag levels were below the detection limit in 4, 2, and 1 samples using Lumipulse-Ag, Lumispot-Ag, and IRMA-Ag kits, respectively (Fig. 2; also, see Fig. S1 in the supplemental material). Significant correlations were observed between assays of HCV core Ag and HCV RNA ($r = 0.9065$ to 0.9666 and $P < 0.0001$ compared with CAP/CTM-RNA data [Fig. 2]); $r = 0.8877$ to 0.9552 and $P < 0.0001$ compared with ART-RNA data [see Fig. S1 in the supplemental material]). The theoretical lower limits of detection of these assays were calculated by use of these correlation formulas and were 3.2 and 3.4 log IU/ml for Architect-Ag, 4.2 and 4.2 log IU/ml for Lumipulse-Ag, 3.7 and 3.9 log IU/ml for Lumispot-Ag, 3.6 and 3.8 log IU/ml for ELISA-Ag, and 3.6 and 3.8 log IU/ml for IRMA-Ag (compared to CAP/CTM-RNA and ART-RNA, respectively). These calculated detection limits were substantially higher than those for the RNA quantitative assays (1.18 and 1.08 log IU/ml for CAP/CTM-RNA and ART-RNA, respectively).

In addition, we found that several samples showed considerable deviation from the linear regression (Fig. 2; also, see Fig. S1 in the supplemental material). To identify the deviating samples, we used Bland-Altman plot analysis (Fig. 3; also, see Fig. S2 in the supplemental material). This plot shows the difference between the titer values of HCV RNA and core Ag as a function of the average of these two values. Several samples demonstrated discordance between the measured HCV RNA and core Ag levels. Among these samples, we focused on samples with discordant results in multiple core Ag assays compared to both RNA quantitative assays. For sample C-01, core Ag levels were underestimated when measured with Architect-Ag, Lumipulse-Ag, and Lumispot-Ag in comparison with CAP/CTM-RNA (Fig. 3) and when measured with Architect-Ag, Lumipulse-Ag, Lumispot-Ag, and IRMA-Ag in comparison with ART-RNA (see Fig. S2 in the supplemental material). Likewise, for sample C-73, core Ag levels were underestimated when measured with Architect-Ag, Lumipulse-Ag, and IRMA-Ag in comparison with CAP/CTM-RNA (Fig. 3) and when measured with Architect-Ag and Lumipulse-Ag in comparison with ART-RNA (see Fig. S2 in the supplemental material). Thus, sample-specific underestimation was observed in several HCV core Ag kits.

Nucleotide sequences in core region of reference panel samples. To clarify the sources of these underestimates of HCV core Ag levels, HCV RNA was extracted from each of the samples in the reference panel, and the nucleotide sequences of core regions were determined. Phylogenetic analysis with these sequences permitted classification of the individual strains by genotype. Of 80 samples in the reference panel, 1 (1.3%) was genotype 1a, 35 (43.8%) were genotype 1b, 26 (32.5%) were genotype 2a, and 18 (22.5%) were genotype 2b (Table 1; also, see Fig. S3 in the supplemental material). These strains were distributed evenly among reference strains of each genotype and cover the sequence diversity of strains isolated in Japan (see Fig. S3 in the supplemental material). The genotypes of samples associated with underestimated core Ag values (samples C-01 and C-73) were both classified as genotype 2a.

Predicted amino acid sequences of HCV core protein were aligned with the consensus core protein sequence for the genotype 1b strains obtained in this study (see Fig. S4 in the supplemental material). Excluding the genotype-specific sequence variations, a specific amino acid polymorphism was identified at amino acid (aa) residue 48 (Ala to Thr) in samples C-01 and C-73. Sample C-01, which yielded underestimated values in most core Ag assays, also possessed an additional polymorphism in the same region,

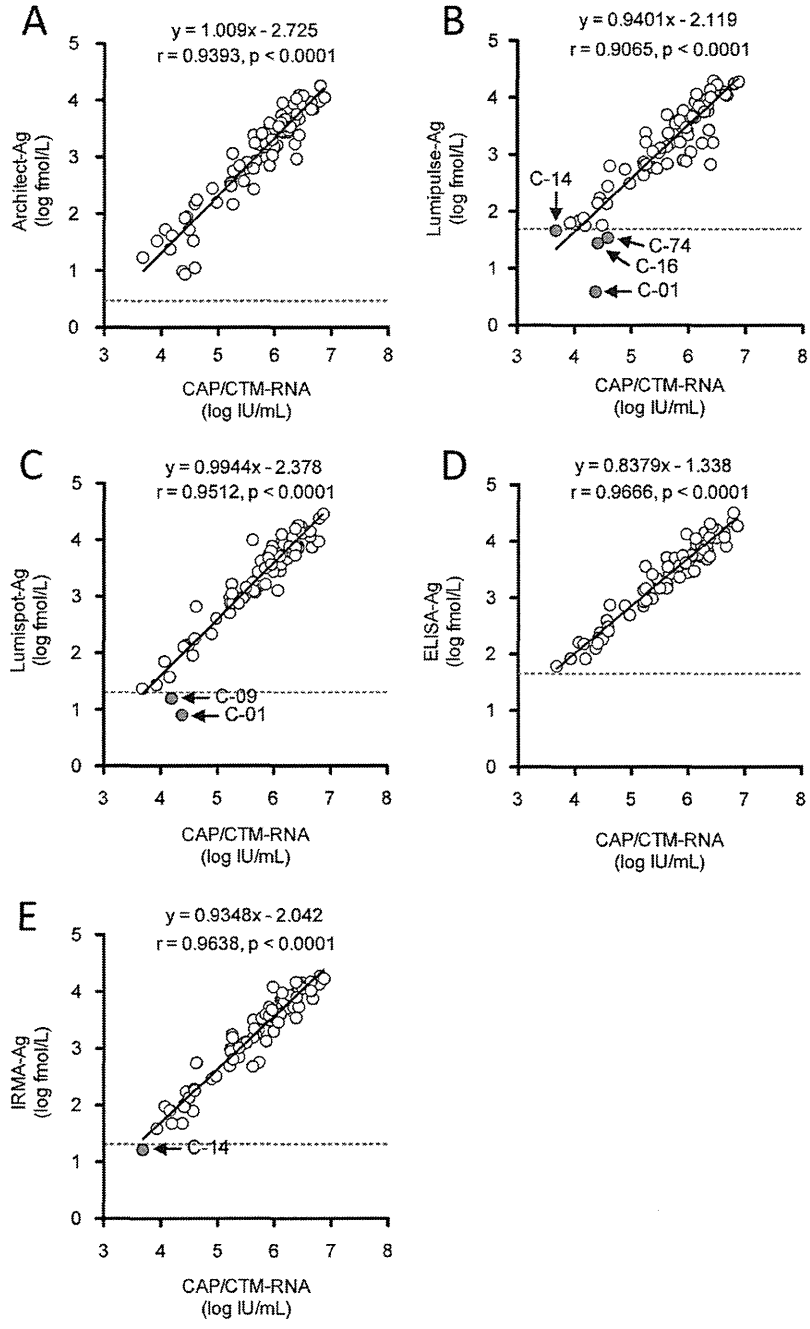

FIG 2 Correlation between CAP/CTM-RNA and core Ag levels as quantified by five commercial kits. Data for core Ag levels were converted to log fmol/liter prior to analysis. In each plot, the lower limit of detection of the respective core Ag assay is indicated by a dotted line. Data for samples below the lower detection limit of each assay are indicated by shaded circles labeled with the respective sample designations.

specifically an Arg-to-Gly substitution at aa 47. We suspected that these polymorphisms altered the antigenicity of the core protein, thereby reducing detected core Ag levels and leading to underestimation of values by the core Ag quantification kits. To assess the correlation of these polymorphisms with the underestimation of core Ag values, strains containing polymorphisms in this region (at aa 47 to 49 [Fig. 4]) were identified in Bland-Altman plots of HCV RNA and core Ag (Fig. 3; also, see Fig. S2 in the supplemental material). A total of 12 strains exhibited polymorphisms at these positions, including 2 strains of genotype 1b, 8 of genotype 2a, and 2 of genotype 2b (Table 1). In the Bland-Altman plot of CAP/CTM-RNA and Architect-Ag, 4 of 12 values (for samples C-01, C-16, C-73, and C-74) were located under the line of the lower 95% limit of agreement (Fig. 3A). Likewise, in the plot of CAP/CTM-RNA and Lumipulse-Ag, 3 of 12 values (those for samples C-01, C-67, and C-73) were located under the line of the lower

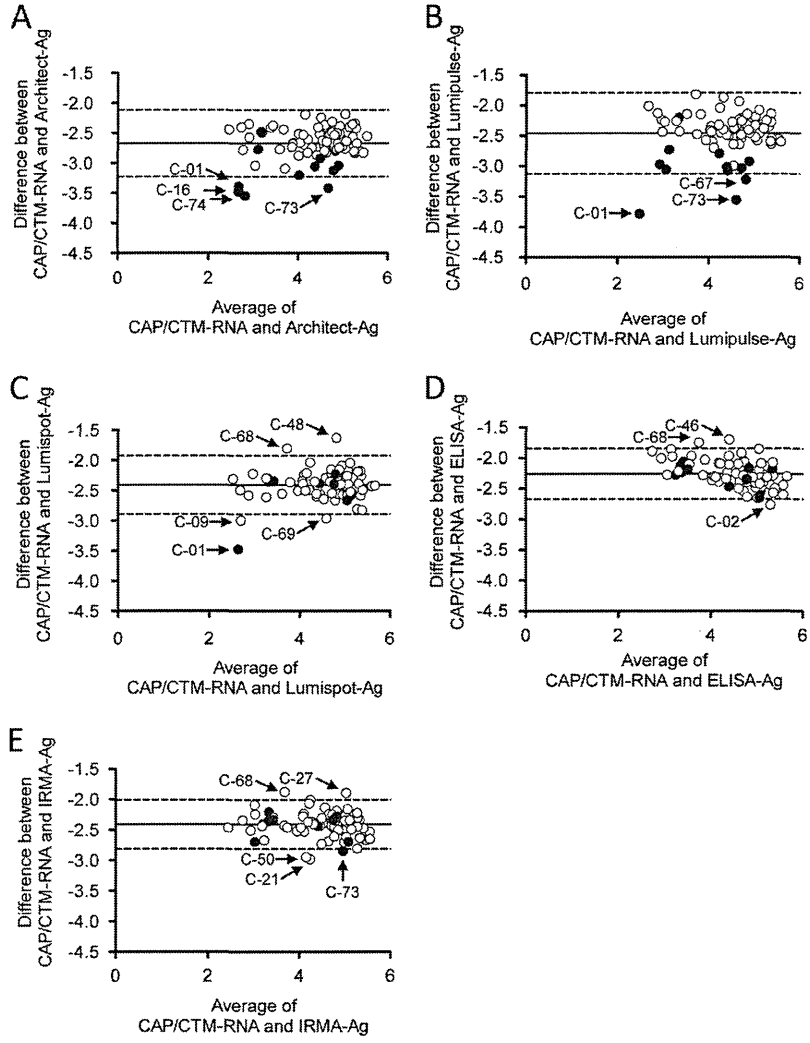

FIG 3 Bland-Altman plot analysis of CAP/CTM-RNA and core Ag levels as quantified by five commercial kits. These plots show the difference between the values of HCV RNA and core Ag as a function of the average of these two values. Data for core Ag levels were converted to log fmol/liter prior to analysis. The bias and 95% limits of agreements are indicated by solid and dashed lines, respectively. Data for samples with polymorphisms at amino acid residues 47 to 49 are indicated by solid circles. Data points outside the 95% limits are indicated by arrows labeled with the sample designations.

95% limit of agreement (Fig. 3B). In these plots, underestimation for samples that lacked these polymorphisms (at aa 47 to 49) was not detected. In the plot of CAP/CTM-RNA and Lumispot-Ag, only 1 sample (C-01) was located under the line of the lower 95% limit of agreement, but this sample exhibited the most discordant value (Fig. 3C). In the plot of CAP/CTM-RNA and ELISA-Ag, no correlation between polymorphisms at these positions and underestimation was observed (Fig. 3D). In the plot of CAP/CTM-RNA and IRMA-Ag, sample C-73 was located under the line of the lower 95% limit of agreement, as were other samples that lacked polymorphisms at aa 47 to 49 (Fig. 3E). Similar trends were observed in comparison with ART-RNA levels (see Fig. S2 in the supplemental material). Based on these results, the levels of HCV core Ag measured with Architect-Ag and Lumipulse-Ag seem to be more strongly affected by single polymorphisms at these positions. In the case of Lumispot-Ag, underestimation may be limited to specimens with multiple polymorphisms at these positions.

TABLE 1 Number of reference panel strains with polymorphisms at amino acid residues 47 to 49 of the HCV core region

Genotype	No. (%) of strains	
	Total	With polymorphisms
1a	1	0
1b	35	2 (5.7)
2a	26	8 (30.8)
2b	18	2 (11.8)
Total	80	12 (15.0)

DISCUSSION

The quantification of HCV viral load is essential for selecting an appropriate antiviral strategy and for monitoring the efficacy of treatment. Since HCV is known to be highly variable and rapidly

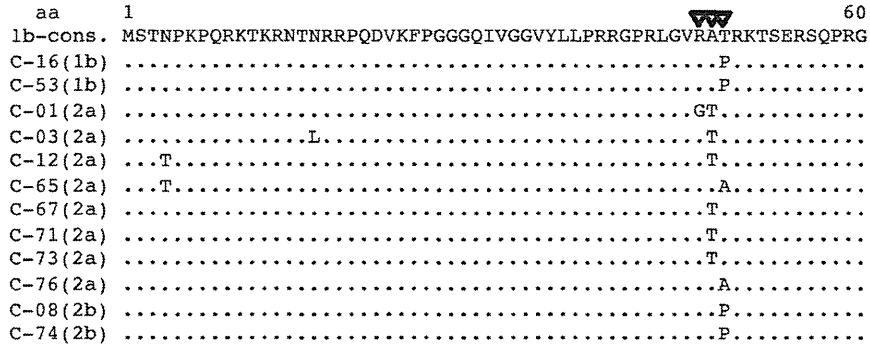

FIG 4 Alignment of the first 60 amino acids of the HCV core region of strains with polymorphisms at amino acid residues 47 to 49. The position numbers are given at the top. Dots indicate identical amino acids. The consensus sequence of 1b strains (1b cons.) isolated in this study was determined and used as a reference sequence. Genotypes of strains are given in parentheses. Positions of polymorphisms are indicated by inverted triangles above the sequence alignment.

evolving (23, 26), the assays for quantifying this virus should be unaffected by sequence polymorphisms. In this study, we established a reference panel with HCV-positive samples and evaluated the correlation among multiple assays for HCV RNA and core Ag quantification.

Using this reference panel, we found that the results from two HCV RNA assay kits, CAP/CTM-RNA and ART-RNA, correlated with excellent agreement ($r = 0.978$, $P < 0.0001$ [Fig. 1]), although discrepancies for values generated by these two assays have been reported for strains of genotypes 1, 2, and 4 (5, 6, 34). In Japan, the prevalent genotypes are 1b, 2a, and 2b (11); no genotype 4 sample was included in our reference panel (Table 1). In quantification with CAP/CTM-RNA, underestimation of HCV RNA titer has been reported for French genotype 2 samples (5). In our panel, no underestimation was observed for data from genotype 2 samples compared to values obtained using ART-RNA. Therefore, underestimation in quantification with CAP/CTM-RNA is expected to be rare in Japanese samples, and the two assays for HCV RNA quantification should be considered accurate and reliable, at least for Japanese samples. Additionally, the prepared reference panel appears to be suitable for the evaluation of HCV quantification assays, because genotypes of samples in this panel are representative of those found in Japan and viral loads are distributed evenly across the range of expected titers.

The quantification of HCV core Ag is an alternative test for HCV infection and viral load. However, in this study, several core Ag quantitative assays failed to provide accurate results for all of the samples in the reference panel (Fig. 2). Some quantified values were below the kits' detection limits. This shortcoming was mainly attributable to the lower sensitivity of the core Ag assay kits; increased sensitivity is urged in the future development of HCV core Ag kits. Among the kits tested here, Architect-Ag assay exhibited the highest sensitivity and was sufficient for quantifying the viral load in all samples. However, even in the case of Architect-Ag, theoretical lower limits of detection, calculated by correlation formula using CAP/CTM-RNA and ART-RNA, were 3.2 and 3.4 log IU/ml, respectively; these detection limits still exceeded the lower limits of the HCV RNA quantification assays. Therefore, the sensitivity of the available HCV core Ag assays is still insufficient to detect low-titer HCV infections. Core Ag kits therefore may be unsuitable for the detection of breakthrough hepatitis during antiviral therapy or for the detection of HCV infection in a window period.

Comparison between HCV RNA and core Ag assays revealed good correlations, with r coefficients ranging from 0.8877 to 0.9666 and P values being less than 0.0001 (Fig. 2; also, see Fig. S1 in the supplemental material). Therefore, the HCV core Ag levels may serve as an alternative to HCV RNA levels when titers remain within the detection ranges of the core Ag kits. However, several discordances were detected when core Ag levels were compared with those of HCV RNA. For one sample in our panel (sample C-01), core Ag levels were lower than expected when quantified using any of the three core Ag kits (Architect-Ag, Lumipulse-Ag, and Lumispot-Ag) (Fig. 3; also, see Fig. S2 in the supplemental material). Another sample (C-73) also yielded lower-than-expected levels when assayed with Architect-Ag and Lumipulse-Ag kits. Sequence analysis of the core region revealed that polymorphisms at aa 47 and 48 correlated with these underestimates by core Ag kits (see Fig. S4 in the supplemental material). These results are consistent with our previous study, which suggested that core Ag levels of HCV strain JFH-1 were underestimated by the Lumipulse-Ag kit in comparison to the ELISA-Ag assay (28). Strain JFH-1 harbors an Ala-to-Thr substitution at aa 48; conversion of Thr to Ala at this position in JFH-1 was sufficient to overcome this underestimation. This region of the core Ag presumably corresponds to one of the epitopes recognized by the monoclonal antibodies used in the Lumipulse-Ag kit, such that polymorphisms at this position affected the antigenicity of the core protein. In this study, we found that the presence of other polymorphisms in this region (aa 47 to 49) correlated with reduced core Ag levels as detected by Lumipulse-Ag, as well as by other assays (Architect-Ag and Lumispot-Ag). Sample C-01 demonstrated a drastic deviation from expected core Ag levels in these assays (Fig. 3; also, see Fig. S2 in the supplemental material). The HCV strain in this sample contains two polymorphisms (Arg to Gly at aa 47 and Ala to Thr at aa 48); the multiple polymorphisms may impair antibody binding more severely and therefore result in underestimation of core Ag levels. Interestingly, this sample exhibited reasonable core Ag levels when assayed using ELISA-Ag. Thus, the underestimation of core protein levels in this sample was kit dependent, suggesting the targeting of distinct epitopes by the antibodies used in each of these kits. This hypothesis could not be confirmed, because the identity of the epitopes targeted by each kit is proprietary.

Of 12 samples with amino acid polymorphisms in this region, 2 (5.7%) were of genotype 1b, 8 (30.8%) were of genotype 2a, and

TABLE 2 Number of strains in the sequence database[a] with polymorphisms at amino acid residues 47 to 49 of the HCV core region

Genotype	No. (%) of strains				
	Tested	With polymorphism			
		At aa 47 (R/C, G)	At aa 48 (A/T, P)	At aa 49 (T/A, P, L)	Total
1b	543	2 (0.36)	4 (0.74)	16 (2.96)	22 (4.1)
2a	24	0	6 (25.0)	1 (4.2)	7 (29.2)
2b	39	0	0	2 (6.9)	2 (6.9)

[a] http://s2as02.genes.nig.ac.jp/.

2 (11.8%) were of genotype 2b (Table 1). Searches of the Hepatitis Virus Database (http://s2as02.genes.nig.ac.jp/) revealed that corresponding amino acid polymorphisms were observed in 22 of 543 strains (4.1%) of genotype 1b, 7 of 24 strains (29.2%) of genotype 2a, and 2 of 39 strains (6.9%) of genotype 2b (Table 2). These percentages were consistent with our observations in the proposed reference panel. These data (our results and those from the database) clearly indicate that genotype 2a strains are the most frequent source of underestimation of core Ag levels. Notably, our search of the sequence database did not yield any HCV strain with multiple polymorphisms in the region from aa 47 to 49, as we saw in our sample C-01. Therefore, strains with such multiple polymorphisms are rare so far, but detection of this isolate among donated blood specimens suggests that such HCV strains could be emerging in clinical samples. For patients harboring such strains, HCV viral load may be underestimated if measurement of HCV viral load is performed by core Ag assay. Such underestimates may result in erroneous selection of therapy, adversely affecting patient outcome. Thus, this shortcoming in HCV core Ag assay kits needs to be addressed.

There is a growing need for evaluation of clinical assay kits with domestic specimen reference panels, since the performance of these kits may be affected by the genotypes or polymorphisms of predominant strains in different geographic regions. To our knowledge, such an investigation of HCV clinical assay kits with domestic specimens has not previously been conducted in Japan. The Japanese HCV reference panel described here was generated with plasma samples collected from Japanese volunteers. Each sample was divided into small aliquots, and the panel was prepared in multiple sets. The samples in our HCV reference panel represent the predominant strains and genotypes seen in Japan. We expect that this reference panel will be of use for the development, evaluation, and optimization of HCV assay kits for the Japanese clinical market.

In conclusion, we have established a Japanese reference panel for evaluation of HCV quantification assays. Using this reference panel, we found that two assay kits for HCV RNA could quantify HCV titers concordantly. We also found that the data generated by HCV core Ag assay kits correlated with the results of HCV RNA assays. However, the nominal core Ag levels measured by several kits underestimated actual levels for HCV samples with polymorphisms at aa 47 to 49 of the core Ag. The panel established in this study is expected to be useful for estimating the accuracy of currently available and upcoming HCV assay kits; such quality control is essential for clinical usage of these kits.

ACKNOWLEDGMENTS

This work was performed as part of a project for the preparation of reference panels of infectious disease specimens at the National Institute of Infectious Diseases in Japan. This work was also partly supported by grants-in-aid from the Japan Society for the Promotion of Science; the Ministry of Health, Labor and Welfare of Japan; the Ministry of Education, Culture, Sports, Science and Technology; and the Research on Health Sciences Focusing on Drug Innovation from the Japan Health Sciences Foundation.

We are grateful to Shun-ya Momose, Shigeharu Uchida, and Satoru Hino (Blood Service Headquarters, Japanese Red Cross Society) for providing specimens, to Tetsuro Suzuki (Department of Infectious Diseases, Hamamatsu University School of Medicine) for contribution to establish the reference panel, and to Kazuo Kobayashi and Masashi Tatsumi (the Committee of the Reference Panels of Infectious Disease Specimens at the National Institute of Infectious Diseases in Japan) for their helpful suggestions. We also thank the manufacturers of HCV quantification kits, including Roche Diagnostics (Tokyo, Japan), Abbott Japan (Tokyo, Japan), Fujirebio (Tokyo, Japan), Eiken Chemical (Tokyo, Japan), and Ortho Clinical Diagnostics (Tokyo, Japan), for quantification of reference panel samples.

REFERENCES

1. **Alvarez M, Planelles D, Vila E, Montoro J, Franco E.** 2004. Prolonged hepatitis C virus seroconversion in a blood donor, detected by HCV antigen test in parallel with HCV RNA. Vox Sang. **86**:266–267.
2. **Aoyagi K, et al.** 1999. Development of a simple and highly sensitive enzyme immunoassay for hepatitis C virus core antigen. J. Clin. Microbiol. **37**:1802–1808.
3. **Aoyagi K, et al.** 2001. Performance of a conventional enzyme immunoassay for hepatitis C virus core antigen in the early phases of hepatitis C infection. Clin. Lab. **47**:119–127.
4. **Bossler A, et al.** 2011. Performance of the COBAS(R) AmpliPrep/COBAS TaqMan(R) automated system for hepatitis C virus (HCV) quantification in a multi-center comparison. J. Clin. Virol. **50**:100–103.
5. **Chevaliez S, Bouvier-Alias M, Brillet R, Pawlotsky JM.** 2007. Overestimation and underestimation of hepatitis C virus RNA levels in a widely used real-time polymerase chain reaction-based method. Hepatology **46**: 22–31.
6. **Elkady A, et al.** 2010. Performance of two real-time RT-PCR assays for quantitation of hepatitis C virus RNA: evaluation on HCV genotypes 1–4. J. Med. Virol. **82**:1878–1888.
7. **Enomoto M, et al.** 2005. Chemiluminescence enzyme immunoassay for monitoring hepatitis C virus core protein during interferon-alpha2b and ribavirin therapy in patients with genotype 1 and high viral loads. J. Med. Virol. **77**:77–82.
8. **Feld JJ, Hoofnagle JH.** 2005. Mechanism of action of interferon and ribavirin in treatment of hepatitis C. Nature **436**:967–972.
9. **Feld JJ, Liang TJ.** 2006. Hepatitis C—identifying patients with progressive liver injury. Hepatology **43**:S194–S206.
10. **Icardi G, et al.** 2001. Novel approach to reduce the hepatitis C virus (HCV) window period: clinical evaluation of a new enzyme-linked immunosorbent assay for HCV core antigen. J. Clin. Microbiol. **39**:3110–3114.
11. **Ikeda K, et al.** 1996. Hepatitis C virus subtype 3b infection in a hospital in Japan: epidemiological study. J. Gastroenterol. **31**:801–805.
12. **Kaiser T, et al.** 2008. Kinetics of hepatitis C viral RNA and HCV-antigen during dialysis sessions: evidence for differential viral load reduction on dialysis. J. Med. Virol. **80**:1195–1201.
13. **Leary TP, et al.** 2006. A chemiluminescent, magnetic particle-based immunoassay for the detection of hepatitis C virus core antigen in human serum or plasma. J. Med. Virol. **78**:1436–1440.
14. **Liang TJ.** 1998. Combination therapy for hepatitis C infection. N. Engl. J. Med. **339**:1549–1550.
15. **Liang TJ, Rehermann B, Seeff LB, Hoofnagle JH.** 2000. Pathogenesis, natural history, treatment, and prevention of hepatitis C. Ann. Intern. Med. **132**:296–305.
16. **Matsuura K, et al.** 2009. Abbott RealTime hepatitis C virus (HCV) and Roche Cobas AmpliPrep/Cobas TaqMan HCV assays for prediction of sustained virological response to pegylated interferon and ribavirin in chronic hepatitis C patients. J. Clin. Microbiol. **47**:385–389.

17. **Mederacke I, et al.** 2009. Performance and clinical utility of a novel fully automated quantitative HCV-core antigen assay. J. Clin. Virol. **46**:210–215.
18. **Medici MC, et al.** 2011. *Hepatitis C virus core antigen:* analytical performances, correlation with viremia and potential applications of a quantitative, automated immunoassay. J. Clin. Virol. **51**:264–269.
19. **Miedouge M, et al.** 2010. Analytical evaluation of HCV core antigen and interest for HCV screening in haemodialysis patients. J. Clin. Virol. **48**: 18–21.
20. **Morota K, et al.** 2009. A new sensitive and automated chemiluminescent microparticle immunoassay for quantitative determination of hepatitis C virus core antigen. J. Virol. Methods **157**:8–14.
21. **Moscato GA, et al.** 2011. Quantitative determination of hepatitis C core antigen in therapy monitoring for chronic hepatitis C. Intervirology **54**: 61–65.
22. **Nubling CM, Unger G, Chudy M, Raia S, Lower J.** 2002. Sensitivity of HCV core antigen and HCV RNA detection in the early infection phase. Transfusion **42**:1037–1045.
23. **Ogata N, Alter HJ, Miller RH, Purcell RH.** 1991. Nucleotide sequence and mutation rate of the H strain of hepatitis C virus. Proc. Natl. Acad. Sci. U. S. A. **88**:3392–3396.
24. **Park Y, Lee JH, Kim BS, Kim DY, Han KH, Kim HS.** 2010. New automated hepatitis C virus (HCV) core antigen assay as an alternative to real-time PCR for HCV RNA quantification. J. Clin. Microbiol. **48**:2253–2256.
25. **Pawlotsky JM.** 2006. Therapy of hepatitis C: from empiricism to eradication. Hepatology **43**:S207–S220.
26. **Robertson B, et al.** 1998. Classification, nomenclature, and database development for hepatitis C virus (HCV) and related viruses: proposals for standardization. Arch. Virol. **143**:2493–2503.
27. **Ross RS, et al.** 2010. Analytical performance characteristics and clinical utility of a novel assay for total hepatitis C virus core antigen quantification. J. Clin. Microbiol. **48**:1161–1168.
28. **Saeed M, et al.** 2009. *Evaluation of hepatitis C virus core antigen assays in* detecting recombinant viral antigens of various genotypes. J. Clin. Microbiol. **47**:4141–4143.
29. **Seeff LB, Hoofnagle JH.** 2002. National Institutes of Health Consensus Development Conference: management of hepatitis C: 2002. Hepatology **36**:S1–S2.
30. **Takahashi M, Saito H, Higashimoto M, Atsukawa K, Ishii H.** 2005. Benefit of hepatitis C virus core antigen assay in prediction of therapeutic response to interferon and ribavirin combination therapy. J. Clin. Microbiol. **43**:186–191.
31. **Tanaka E, et al.** 2000. Evaluation of a new enzyme immunoassay for hepatitis C virus (HCV) core antigen with clinical sensitivity approximating that of genomic amplification of HCV RNA. Hepatology **32**:388–393.
32. **Tanaka Y, et al.** 2003. High stability of enzyme immunoassay for hepatitis C virus core antigen-evaluation before and after incubation at room temperature. Hepatol. Res. **26**:261–267.
33. **Vermehren J, et al.** 2008. Differences between two real-time PCR-based hepatitis C virus (HCV) assays (RealTime HCV and Cobas AmpliPrep/ Cobas TaqMan) and one signal amplification assay (Versant HCV RNA 3.0) for RNA detection and quantification. J. Clin. Microbiol. **46**:3880–3891.
34. **Vermehren J, et al.** 2011. Development of a second version of the Cobas AmpliPrep/Cobas TaqMan hepatitis C virus quantitative test with improved genotype inclusivity. J. Clin. Microbiol. **49**:3309–3315.
35. **Vermehren J, et al.** 2011. Multi-center evaluation of the Abbott RealTime HCV assay for monitoring patients undergoing antiviral therapy for chronic hepatitis C. J. Clin. Virol. **52**:133–137.

SUPPLEMENTALY MATERIALS

SUPPLEMENTARY FIGURE LEGEND

Supplementary Figure 1.

Correlation between ART-RNA and core Ag levels as quantified by five commercial kits. Data for core Ag levels were converted to log fmol/L prior to analysis. In each plot, the lower limit of detection of the respective core Ag assay is indicated by a dotted line, and the respective correlation coefficient and formula are provided at the top of each plot. Data for samples below the lower detection limit of each assay are indicated by shaded (gray) circles, and sample designations are indicated by arrows.

Supplementary Figure 2.

Bland-Altman plot analysis of ART-RNA and core Ag levels as quantified by five commercial kits. These plots show the difference between the

values of HCV RNA and core Ag as a function of the average of these two values. Data for core Ag levels were converted to log fmol/L prior to analysis. The bias and 95% limits of agreements are indicated by bold and dashed lines, respectively. Data for samples with polymorphisms at amino acid residues 47 – 49 are indicated by closed (black) circles. Sample designations for samples outside the 95% limits are indicated by arrows.

Supplementary Figure 3.

The phylogenetic tree constructed with sequences determined in this study. This phylogenetic tree contains 80 strains in the reference panel, reference strains submitted from Japan (24 strains of genotype 1b, 19 strains of genotype 2a, and 25 strains of genotype 2b), and 7 representative strains of each genotype (H77; genotype 1a, Con1, BK, and Taiwan; genotype 1b, BEBE1; genotype 2c, K3a; genotype 3a, and ED43; genotype 4a). The genetic distances were calculated by 6-parameter method, and a phylogenetic tree was constructed by neighbor-joining method by use of software in Hepatitis Virus

Database (http://s2as02.genes.nig.ac.jp/). The length of horizontal bars indicates the numbers of nucleotide substitutions per site.

Supplementary Figure 4.

Alignment of deduced amino acids in the HCV core region. The position number of the amino acids is indicated at both ends of each sequence. Dots indicate identical amino acids. The consensus sequence of 1b strains (1b cons.) isolated in this study was determined and used as a reference sequence. Genotypes of strains in alignment are indicated in parentheses. Strains with discordance in multiple core Ag assays as compared with both RNA quantitative assays are indicated in bold lettering (C-01 and C-73).

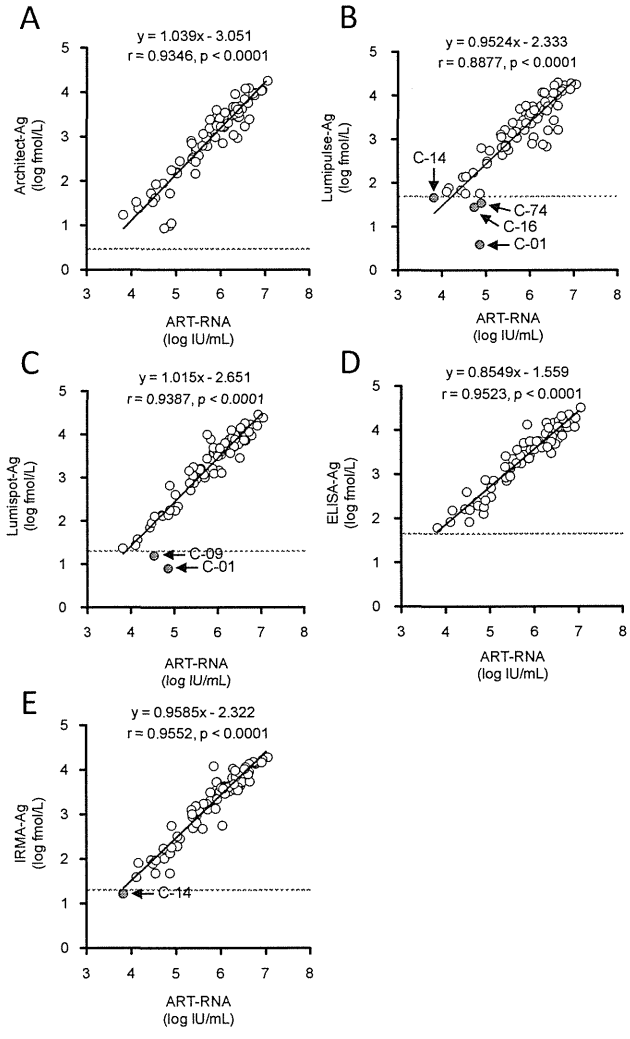

Supplementary Figure 1